Downwind Development in a Stationary Band Complex Leading to the Secondary Eyewall Formation in the Simulated Typhoon Soudelor (2015)

Xue-Song Zhu, Hui Yu, and Yuqing Wang

MWR 2022

Introduction

- Intense TCs often develop a secondary eyewall.
- Mechanisms leaded to SEF:
  - VRWs: VRWs propagate radially outward to a stagnation radius. The wave kinetic energy is converted to the tangential wind by wave-mean flow interaction. Then, the wind enhance surface enthalpy flux and initiate convection. (Montgomery and Kallenbach 1997; Mong and Emanuel 2003)
  - Unbalanced dynamics: BL inflow induced by outer rainband can sharpen the radial wind gradient and create strong supergradient wind. Broadening of the tangential wind induces the unbalanced outflow just above the BL and then develops the axisymmetric secondary eyewall. (Qiu and Tan 2013; Huang et al. 2012; Abarca and Montgomery 2013, 2014)
  - Balanced dynamics: Strong diabatic heating in outer rainbands and high environmental RH can broaden the tangential wind outside the primary eyewall. Diabatic heating from stratiform precipitation is more effective in producing a secondary wind maximum than that form convective precipitation. (Wang 2009; Rozoff et al. 201; Moon and Nolan 2010)
  - Large scale interaction: Interaction between a TC and a midlatitude westerly jet can produce stratiform precipitation with embedded deep convection and evolve into the secondary eyewall finally. (Dai et al. 2017)

Introduction

- Asymmetric rainbands in SEF:
  - Downward and inward development of an intense outer rainband and associated inflow (MDI) led to the associated strong tangential wind above BL. (Wang et al. 2019)
  - When reaching the outer edge of the rapid filamentation zone, the tangential wind jet is effective axisymmetrized. The secondary tangential wind maximum and convective ring formed sequentially.
  - MDI initiated in the stratiform precipitation region can descend into the BL and trigger an intense updraft. The associated secondary circulation can accelerate the tangential wind. (Didlake et al. 2018; Yu et al. 2021; Wang and Tan 2020)

Introduction

- Not all outer rainbands propagate radially inward and lead to SEF.
- Stationary band complex (SBC): wavenumver-1 asymmetry and quasi-stationary relative to the TC.
- In a statistical analysis of 5-year microwave satellite observations:
  - 6 hours prior to SEF: 79% of the 84 SEF cases had SBC.
  - 12 hours prior to SEF: SBC becomes more tangential and axisymmetrization.

(Vaughan et al. 2020)

- Objective:
  - The evolution from spiral rainband to a SBC
  - How the SBC contributes to the convective onset in SEF?

WRF Configuration

Version	3.8.1
Domains	3, d02 and d03 are moving
Grid size	18, 6, 2 (km)
Start time	2015-08-01 1200 Z
End time	2019-08-07 1200 Z
Eta levels	36 (8 levels in z < 1.5 km)
Model top	20 hPa
Cumulus Scheme	Kain-Fritsch (d01 only)
Microphysics Scheme	NSSL two-moment
Longwave Scheme	RRTM
Shortwave Scheme	RRTM
PBL Scheme	YSU
Land surface scheme	Noah
DATASET resolution	0.25° x 0.25°
DATASET	NCEP GFS FNL

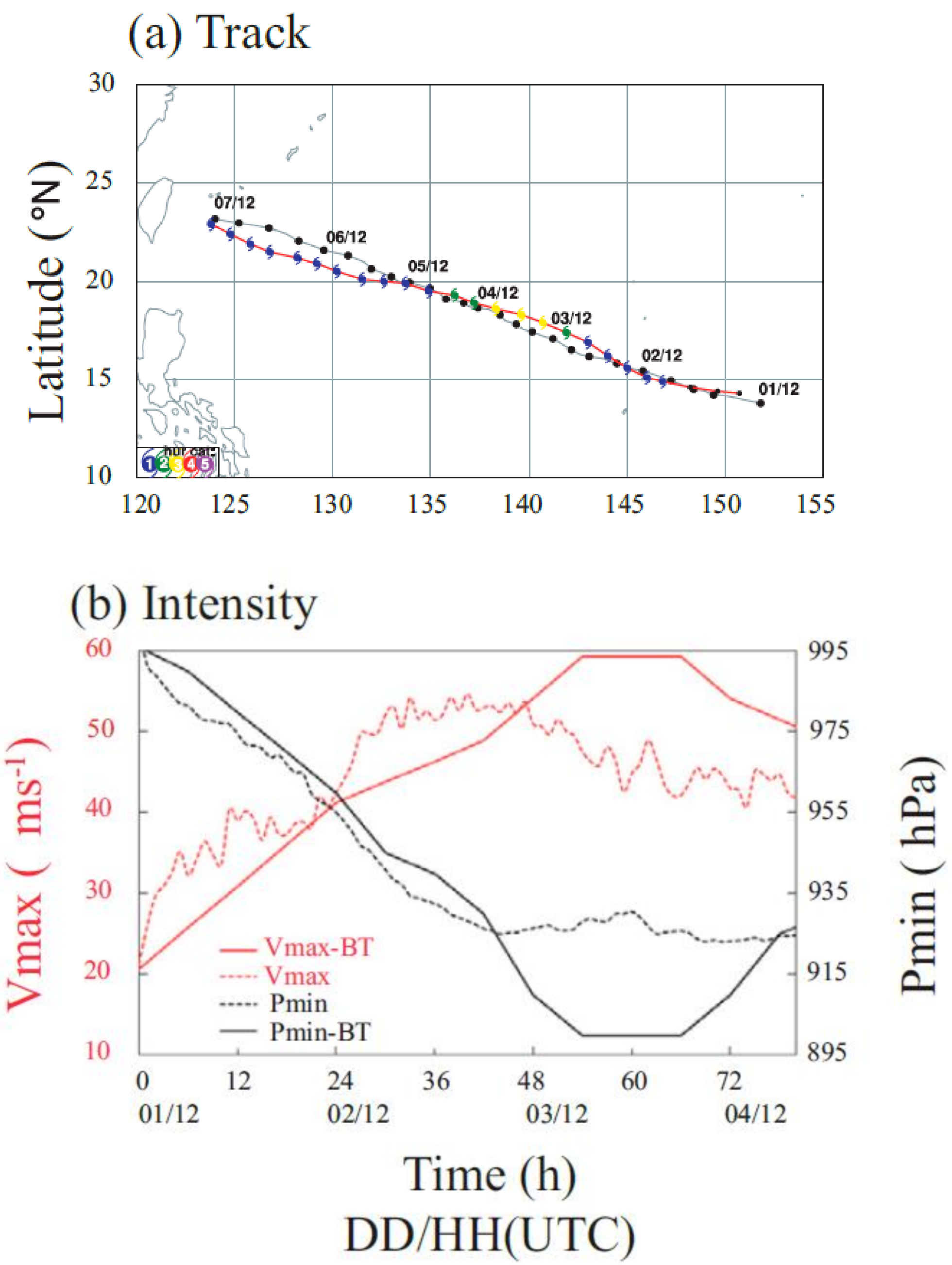

All horizontal wind in this study are storm-relative.

Simulation results

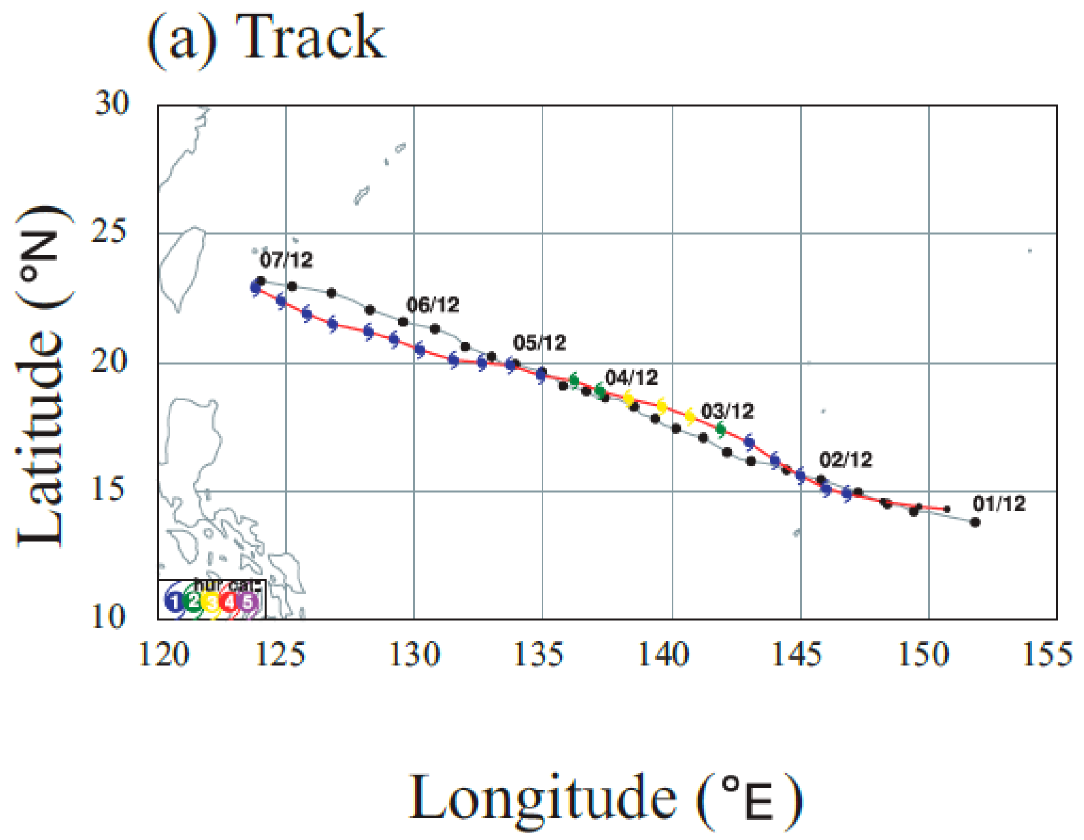

Simulated track and JMA best track

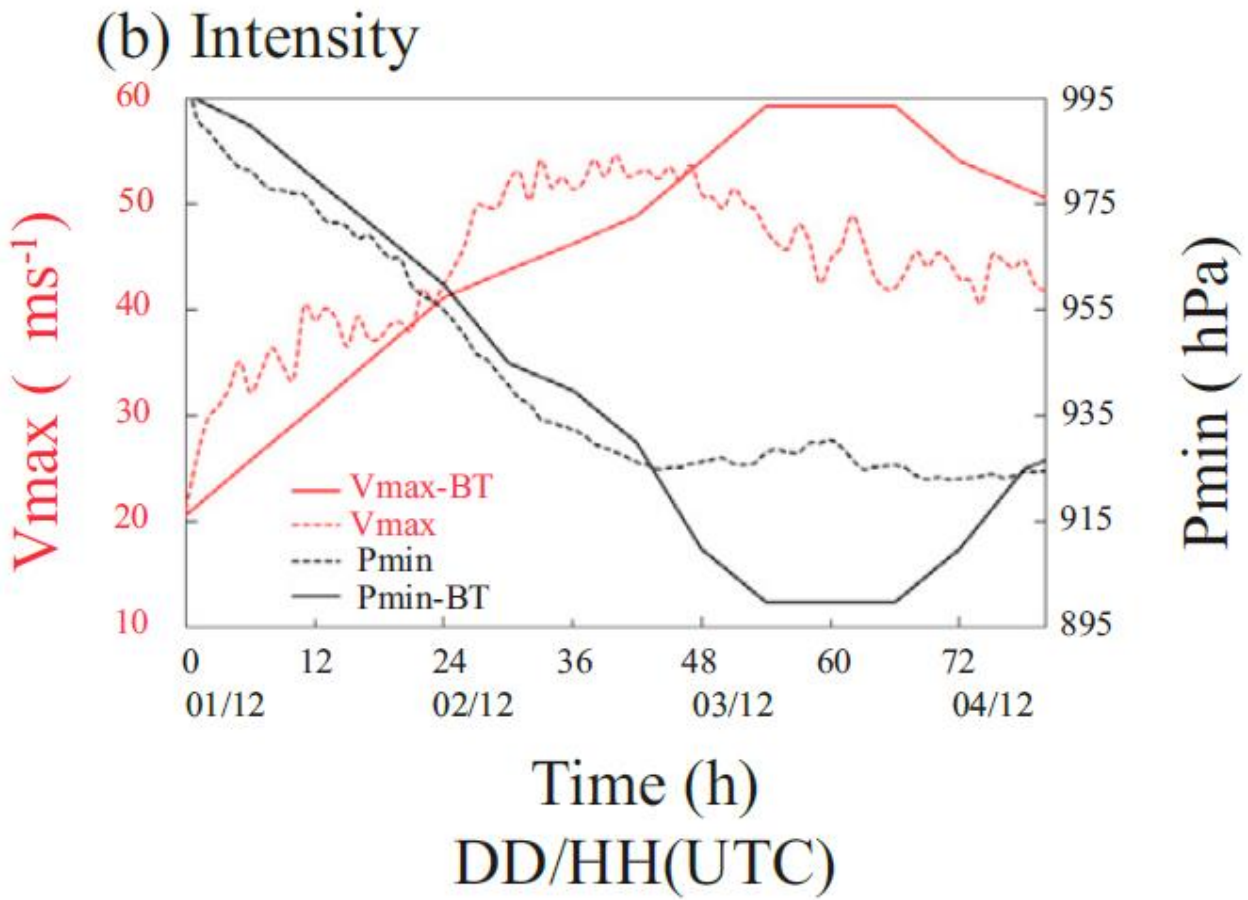

	Simulation	Best-track
10-m Vmax		
Sea level P		

Plan view of simulated Soudelor

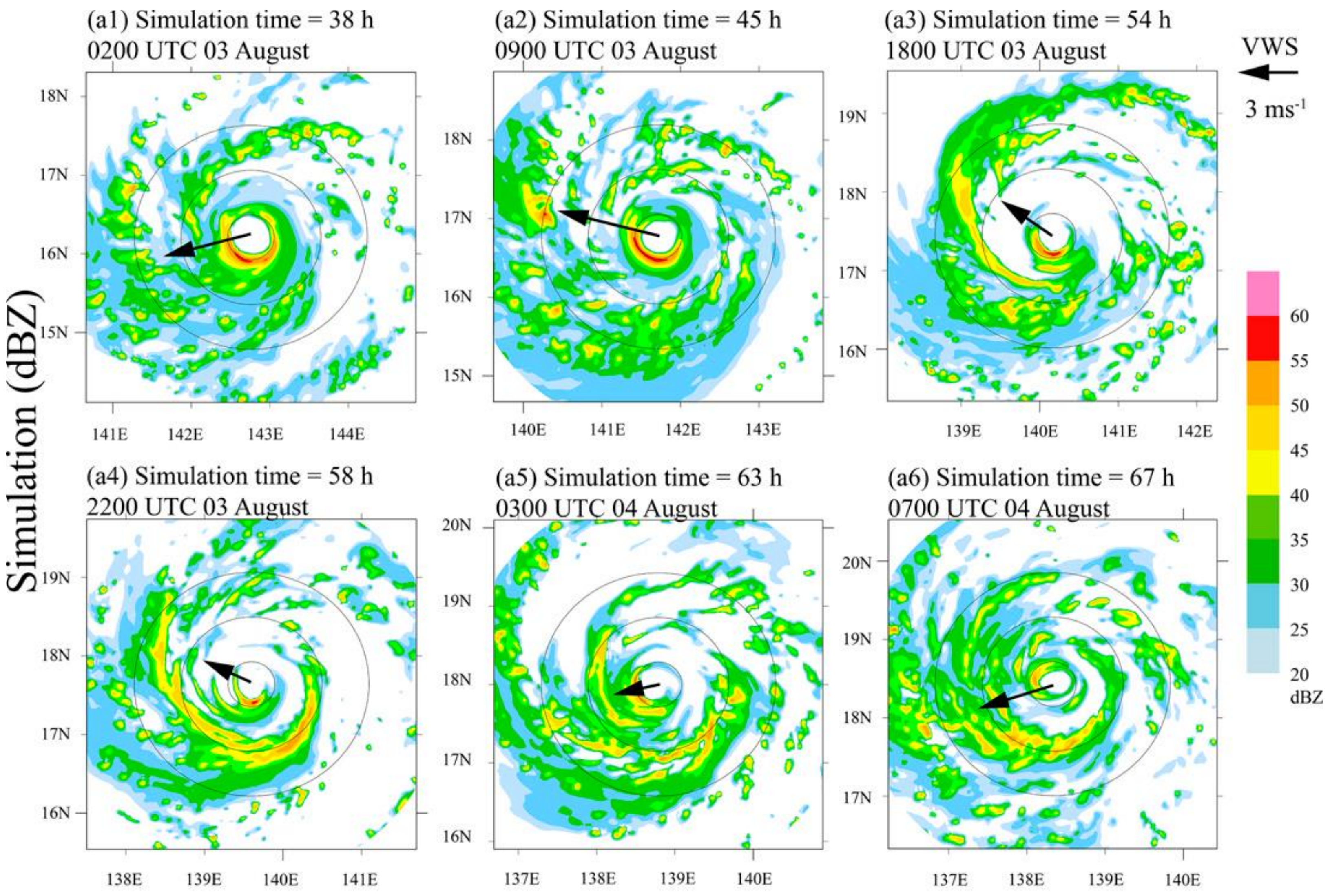

Z = 3 km
Colored: reflectivity (dBZ)
Arrow: VWS (m/s)
Circle: 30, 90, 150 km
from TC center

Vertical wind shear (VWS): Difference between 200 and 850 hPa of averaged wind speed in r = 200-800 km annular area.

Plan view of simulated Soudelor

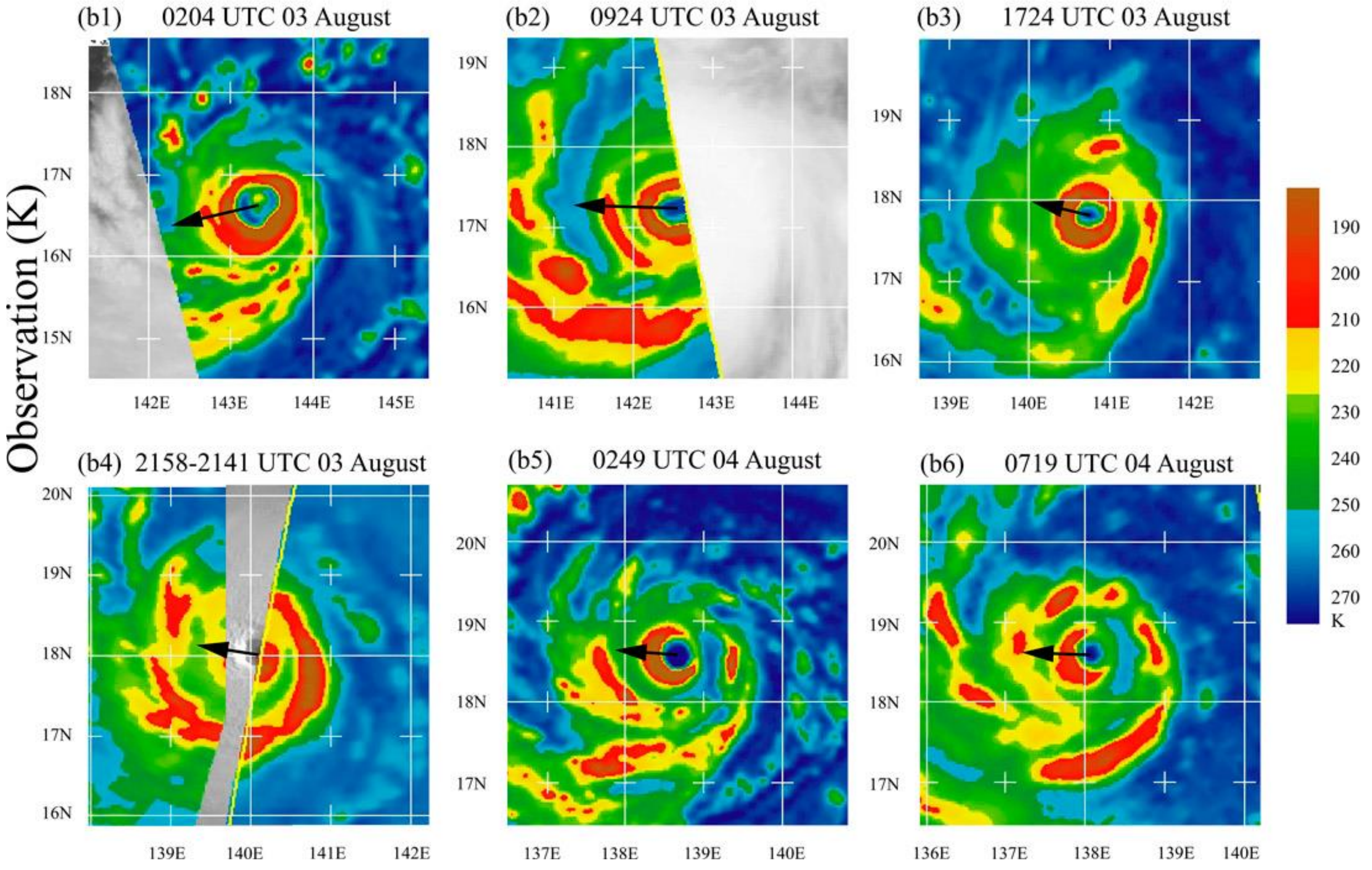

Colored: Brightness temperature (K)
Arrow: VWS (m/s)

Vertical wind shear (VWS): Difference between 200 and 850 hPa of averaged wind speed in r = 200-800 km annular area.

Azimuthal mean

Azimuthal-mean
Colored: w (m/s)
Contour: v (m/s)
Arrow: u, w (m/s)

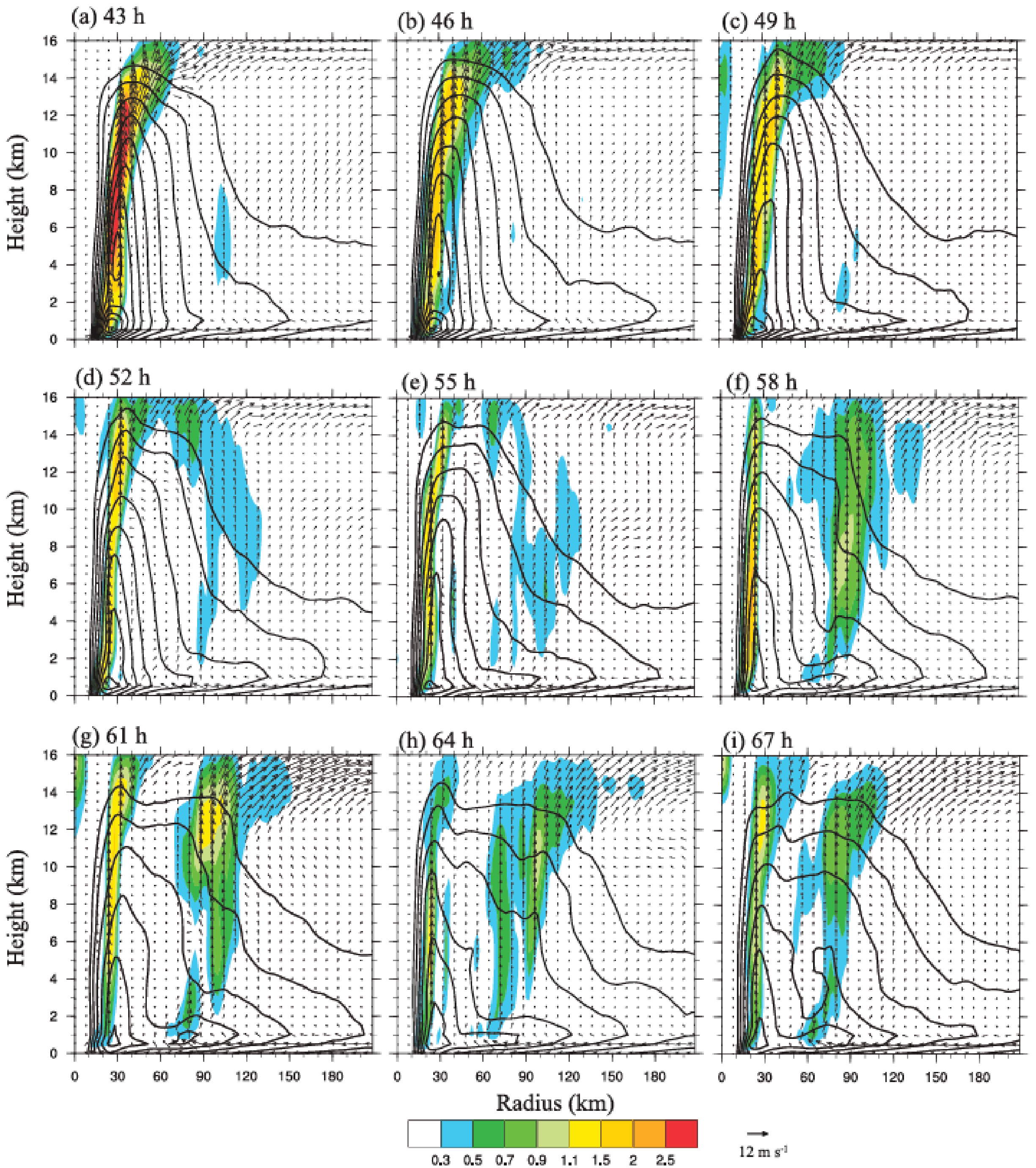

Azimuthal mean

Azimuthal-mean
Colored: w (m/s) at z = 3 – 7 km
Contour: v (m/s) at z = 0.6 km

Middle-level updraft > 0.5 m/s outside the eyewall implies the strengthening of rainband convection. (Rozoff et al. 2012)

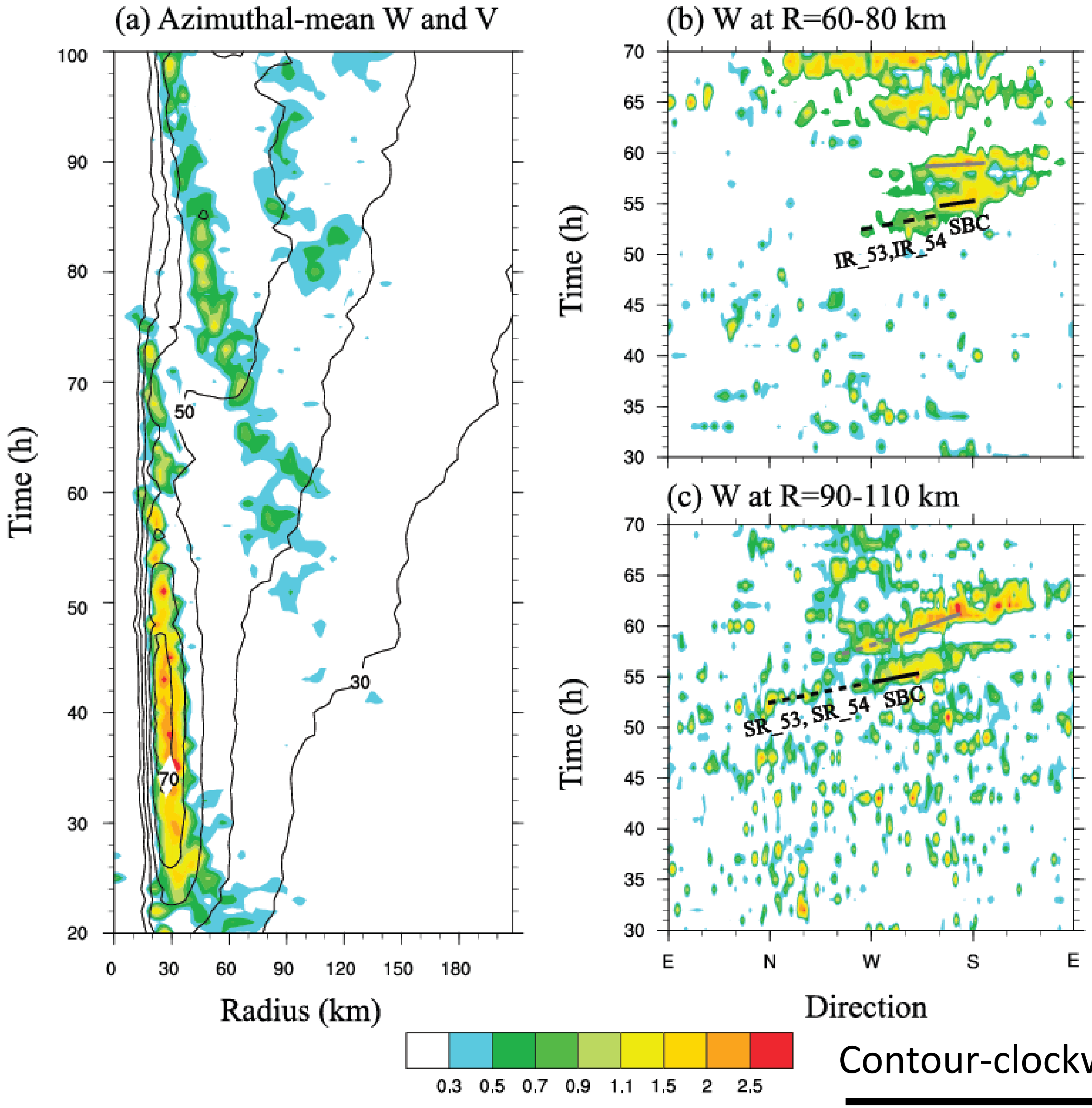

Contour-clockwise

Analysis of SBC (53h)

Color: dBZ
at z = 3 km

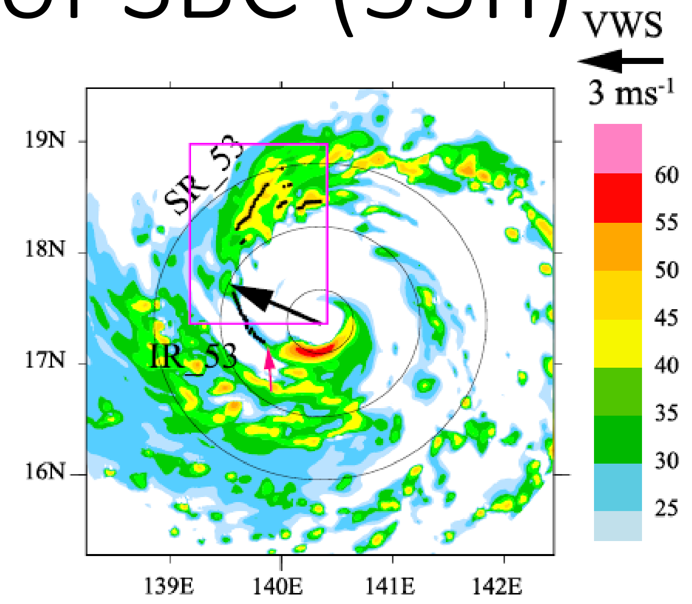

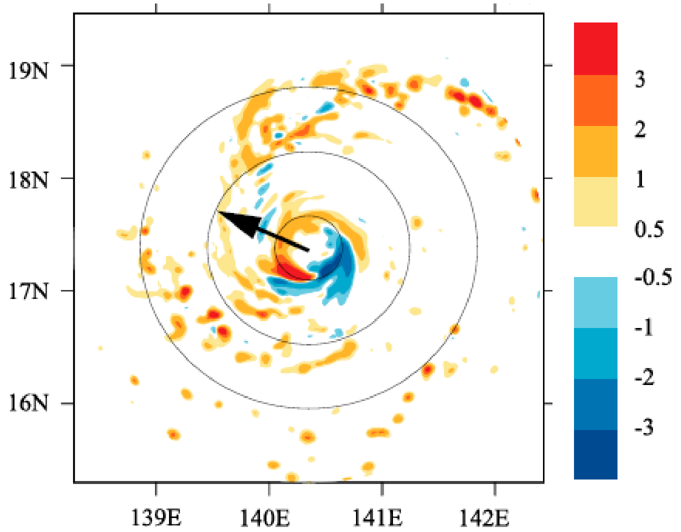

Color: w
at z = 3 - 7 km

Color: divergence
at z = 3 km
Contour: w
at z = 3 -7 km

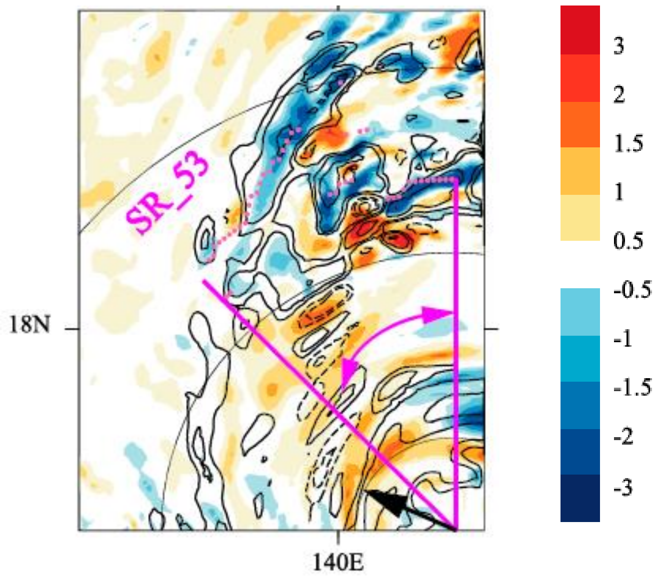

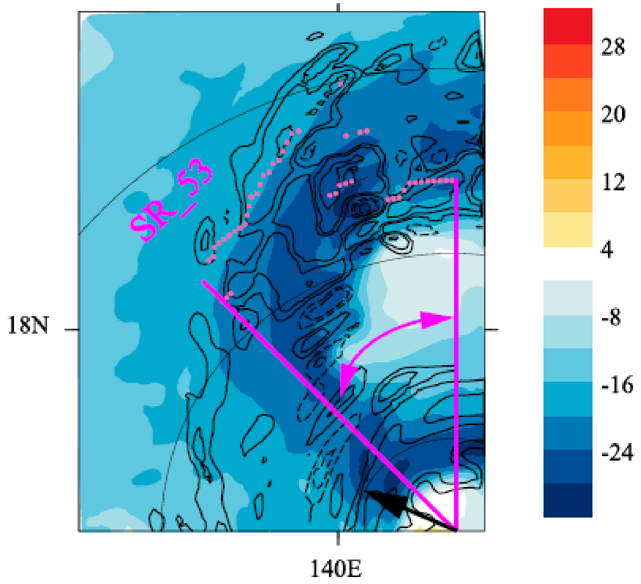

Color: u
at z = 0.3 km
Contour: w
at z = 3 -7 km

Analysis of SBC (54h)

Color: dBZ
at z = 3 km

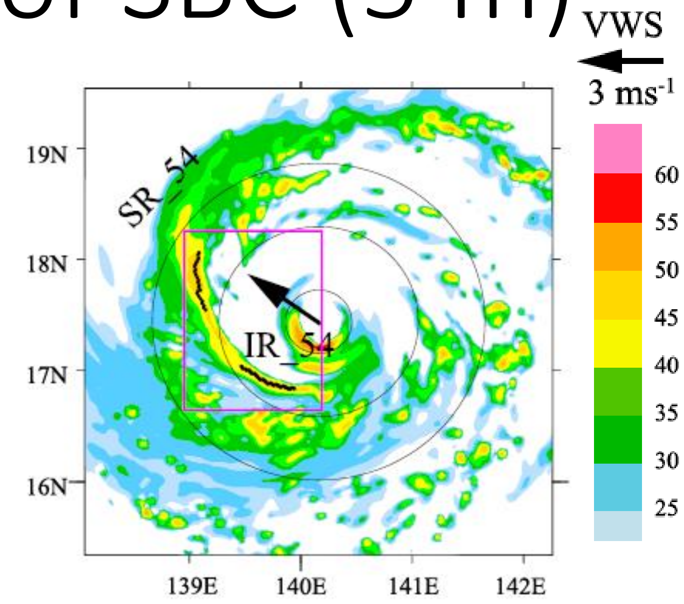

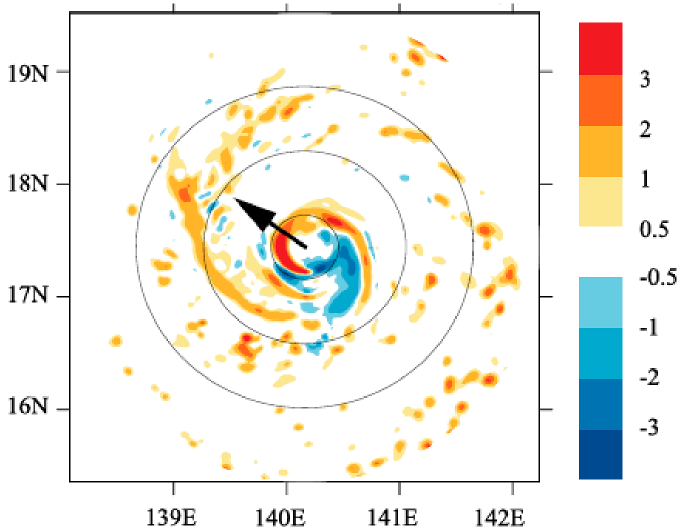

Color: w
at z = 3 - 7 km

Color: divergence
at z = 3 km
Contour: w
at z = 3 -7 km

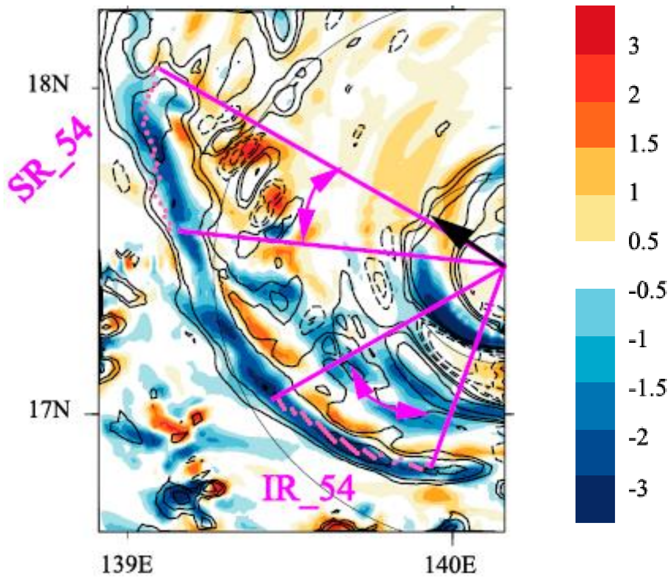

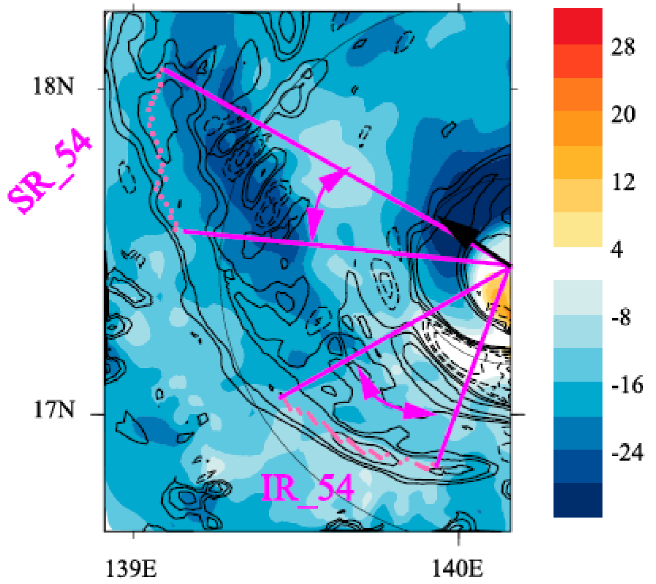

Color: u
at z = 0.3 km
Contour: w
at z = 3 -7 km

Analysis of SBC (55h)

Color: dBZ
at z = 3 km

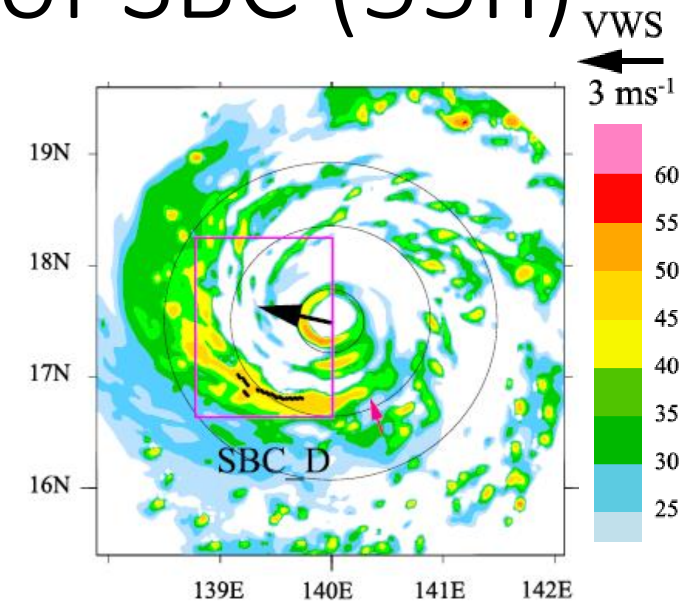

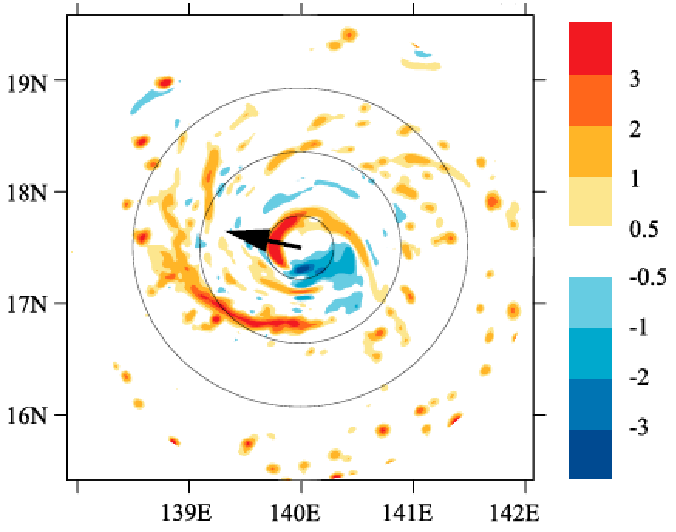

Color: w
at z = 3 - 7 km

Color: divergence
at z = 3 km
Contour: w
at z = 3 -7 km

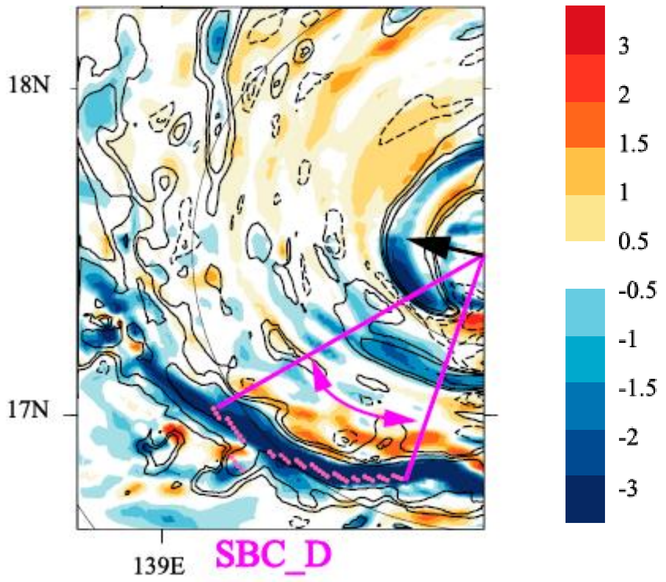

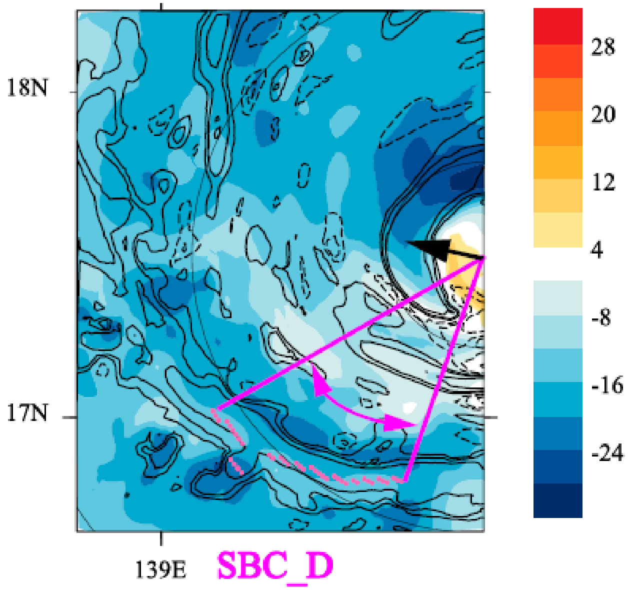

Color: u
at z = 0.3 km
Contour: w
at z = 3 -7 km

Cross section of SBC

Line-averaged
Color: dBZ
Vector: u, w
Contour: w
Contour: v’

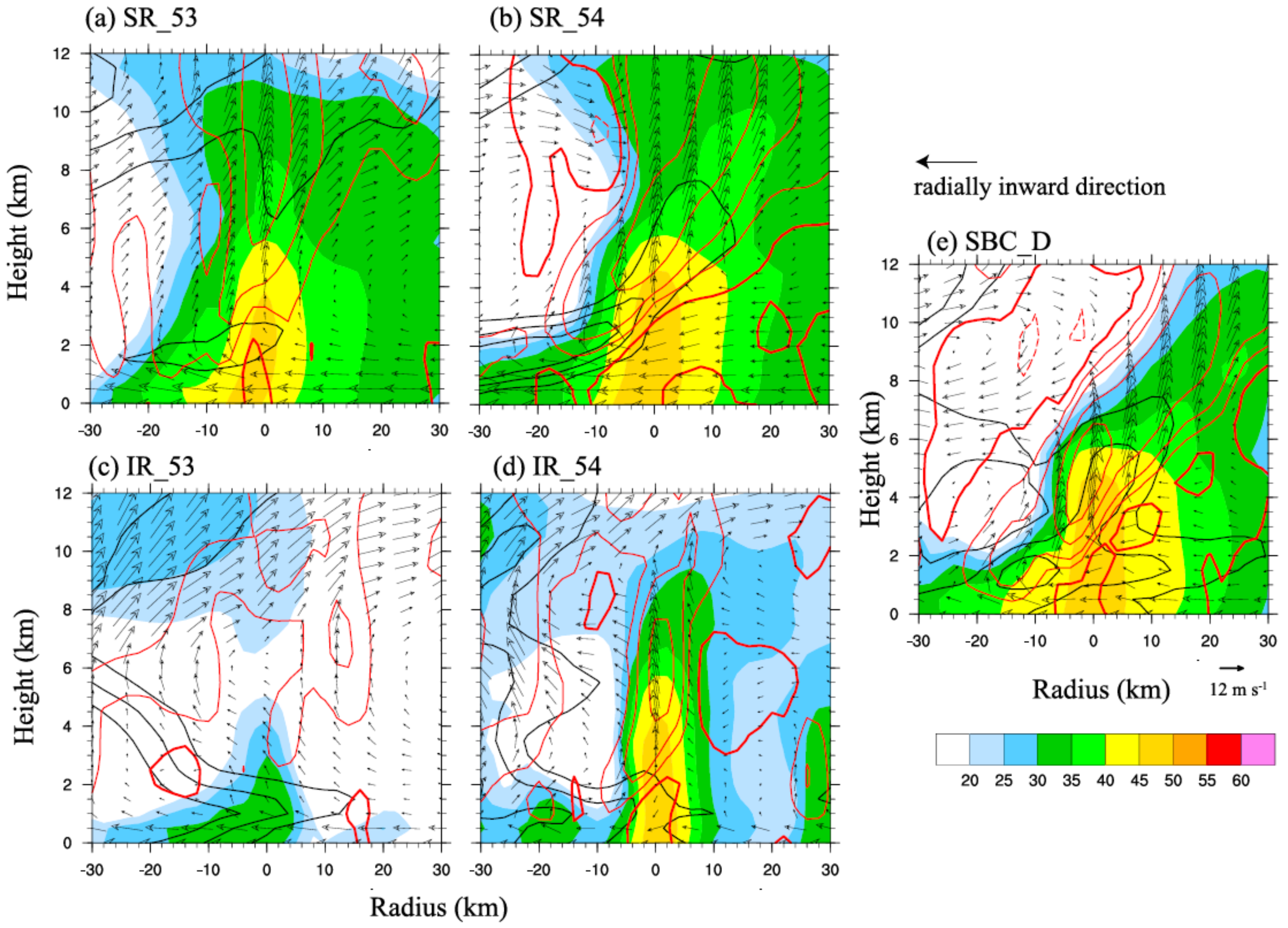

Cross section of SBC

Line-averaged
Color: θ_e
Vector: u, w
Contour: qr
Contour: qv
Dashed Contour: RH

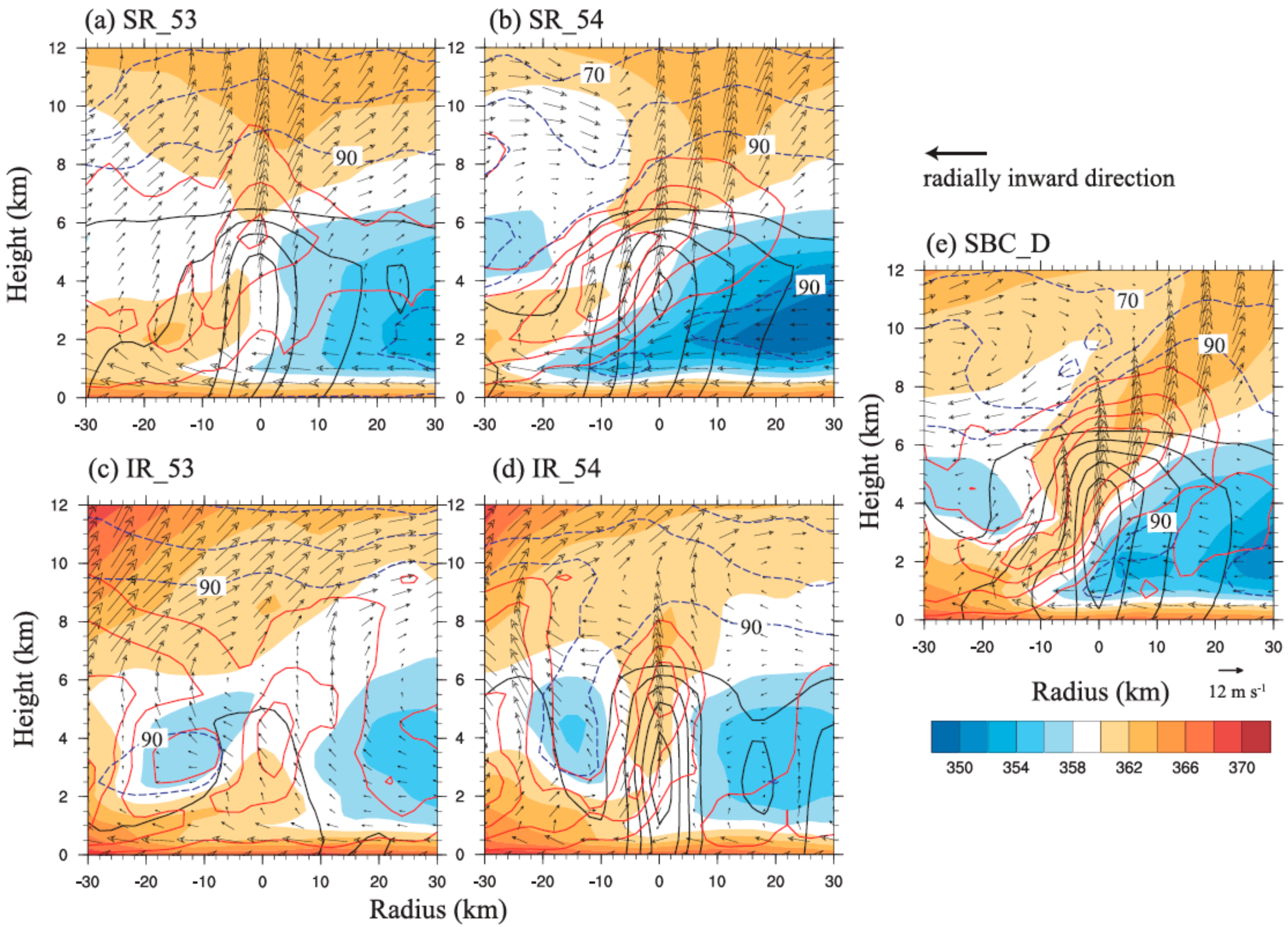

Supergradient force

Line-averaged
Color: divergence
Vector: u, w
Contour: w
Contour: AF

$$\mathrm{AF} = f v + \frac{v^2}{r} - \frac{1}{\rho}\frac{\partial p}{\partial r},$$

Agradient force (AF)
AF > 0 supergradient wind
AF < 0 subgradient wind

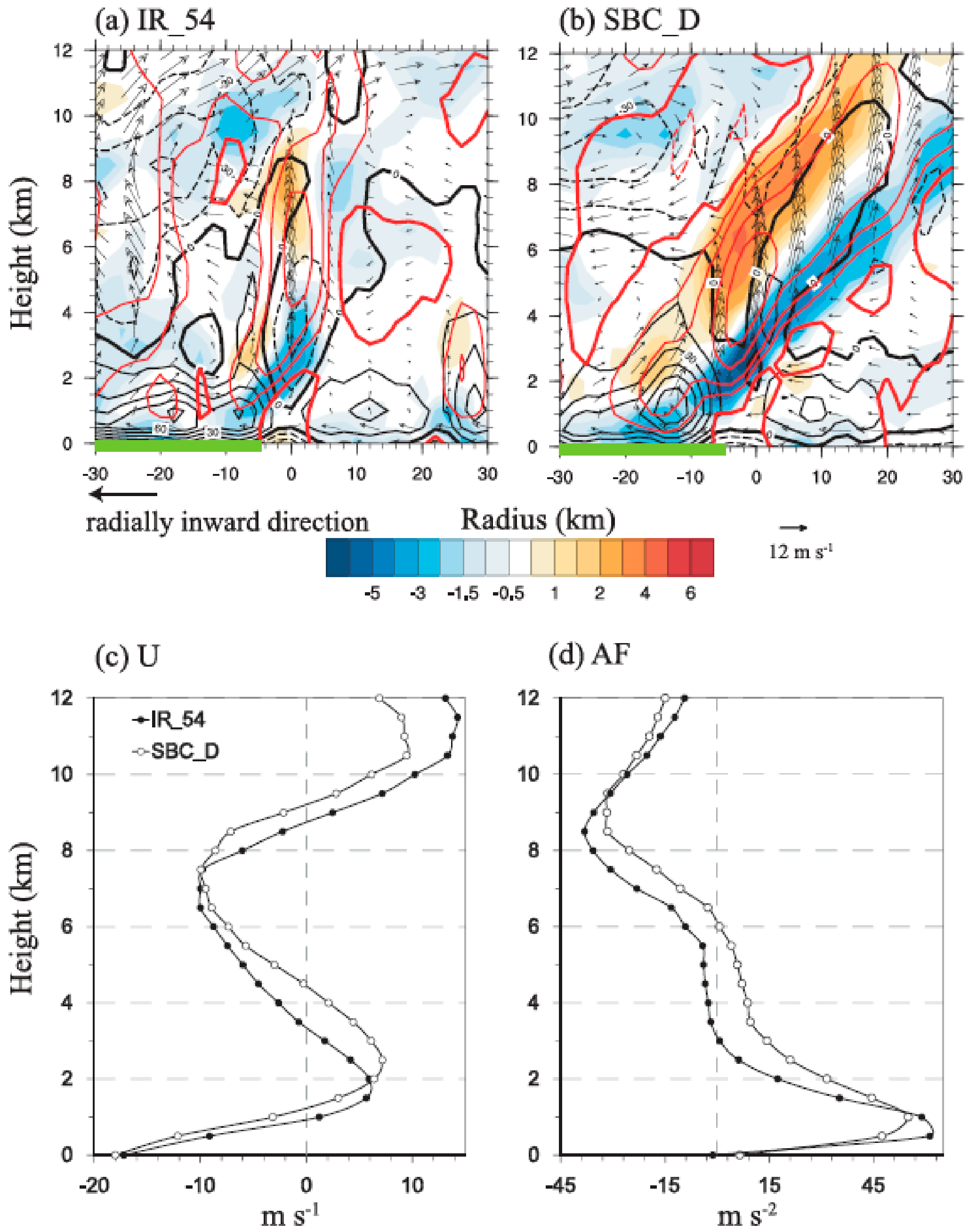

Propagation speed of IR

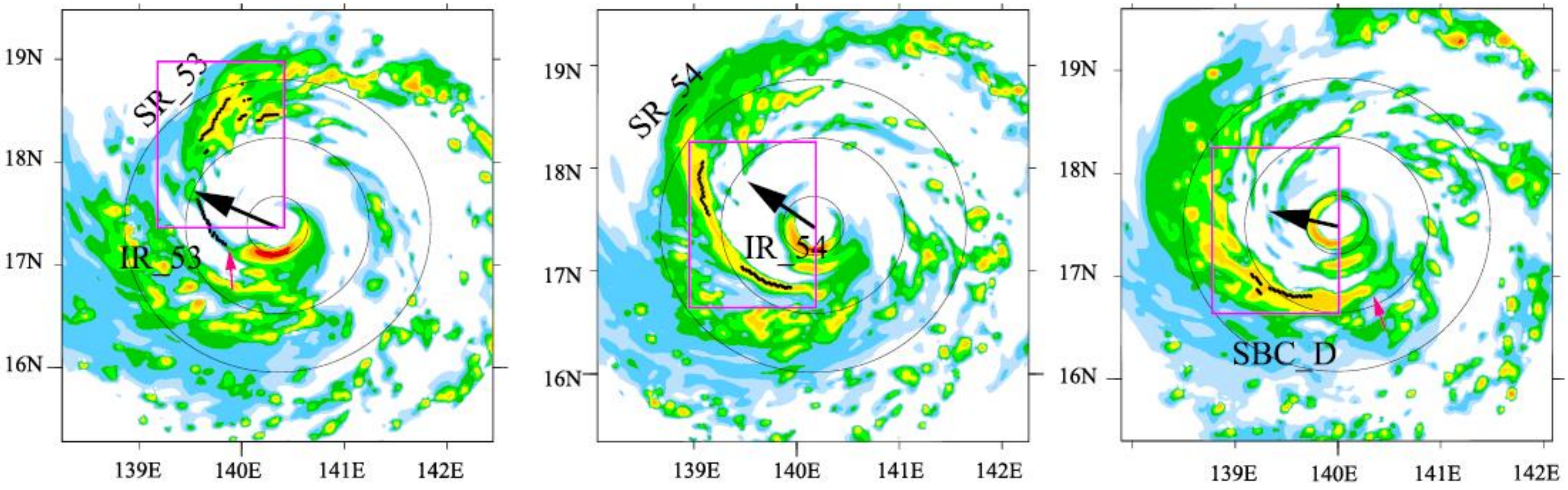

Average radial propagation speed of IR: 2.4 m/s   65 km -> 73 km -> 82 km

Average tangential propagation speed of IR: 17.3 m/s   (43% of tangential wind)

Low-level outflow: 1.6 m/s

Tangential propagation speed associated with VRWs: 60 ~ 80% of tangential wind

Budget analysis of AF

$$\mathrm{AF} = fv + \frac{v^2}{r} - \frac{1}{\rho}\frac{\partial p}{\partial r},$$

AF_O   AF_I

Contour: w at z = 1 km
Red dot: max dBZ

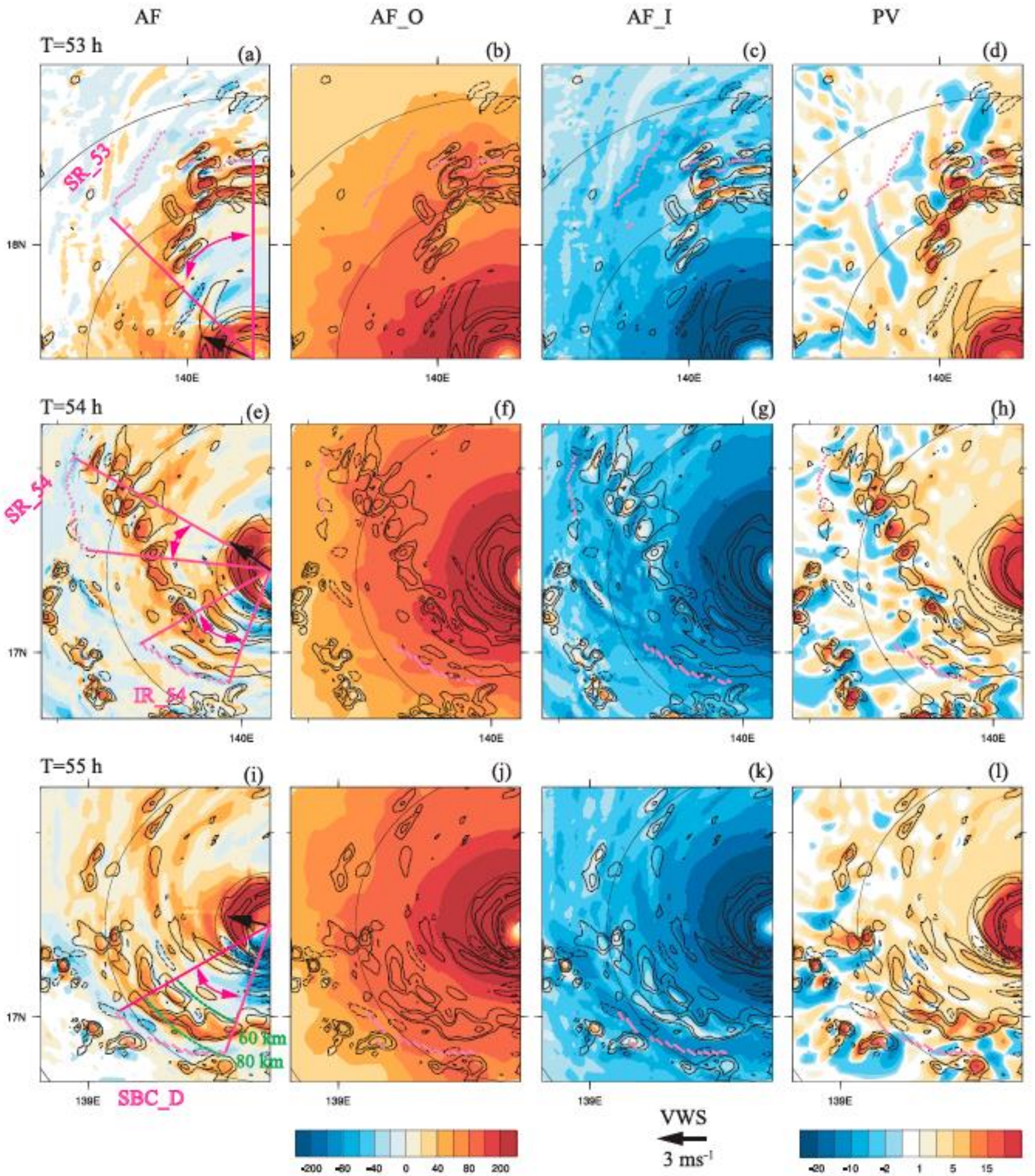

Budget analysis of AF

r = 60 – 80 km
SBC sector average AF

r = 60 – 80 km
Axisymmetric AF

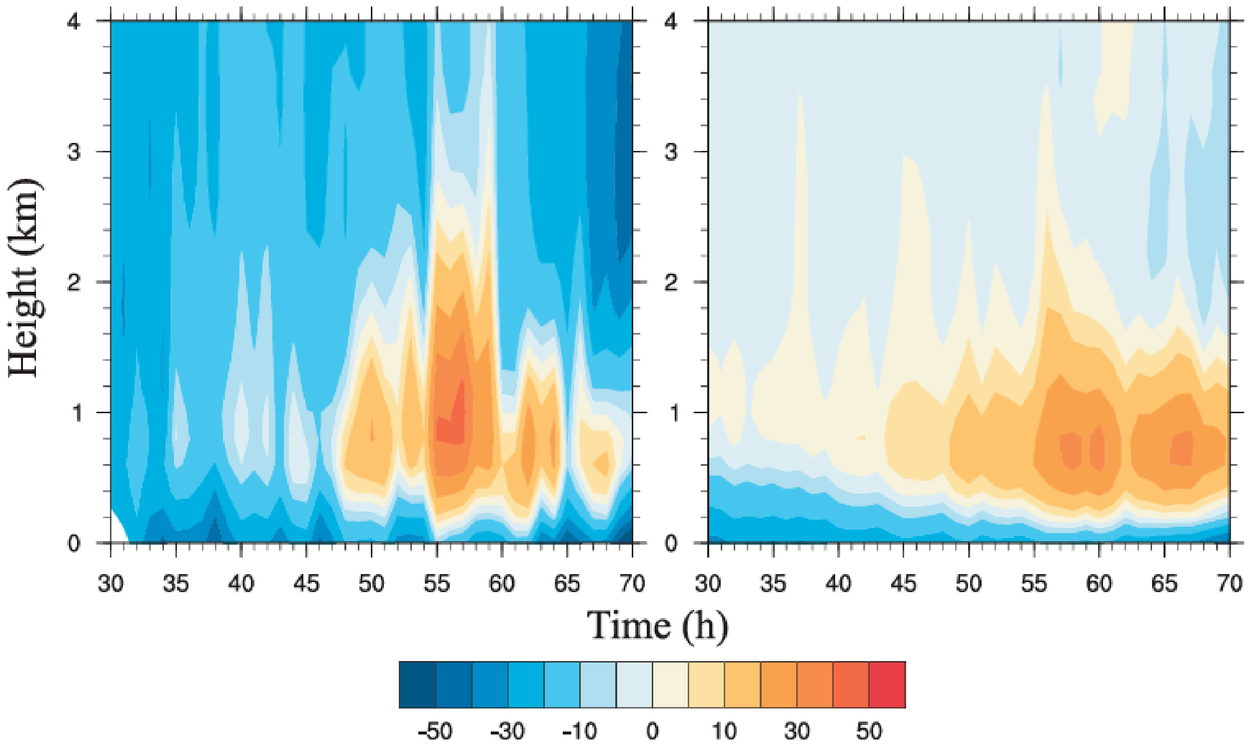

r = 60 – 80 km
z = 700 average

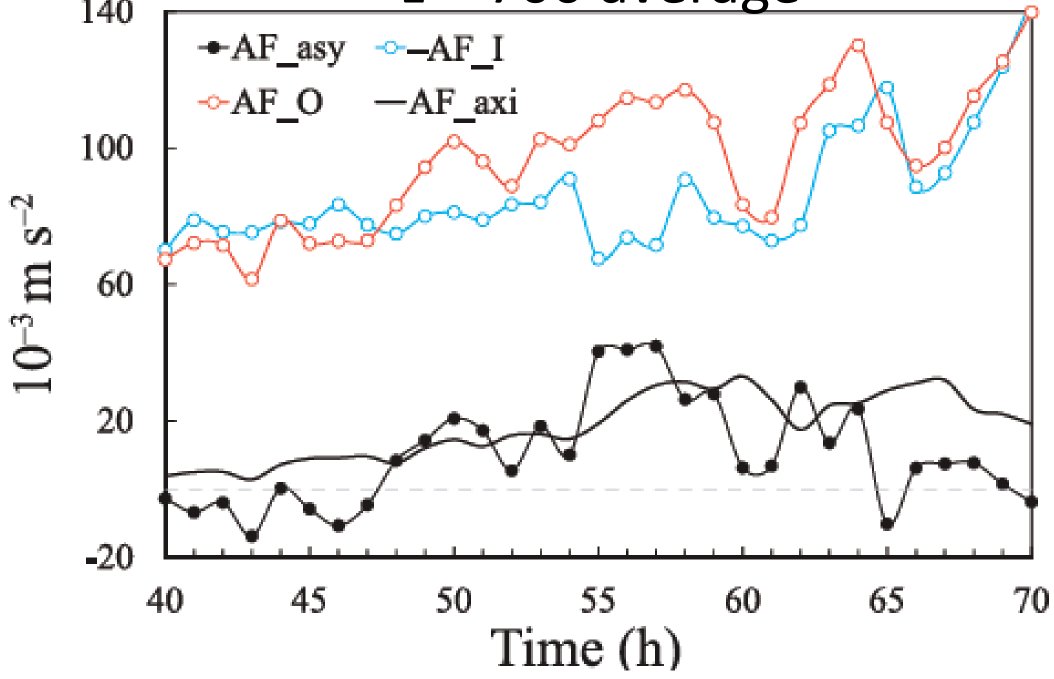

Cold pool formation in the downwind propagation

$\bar{\phi} = mean(\phi_{-12.5}, \phi_{+12.5})$

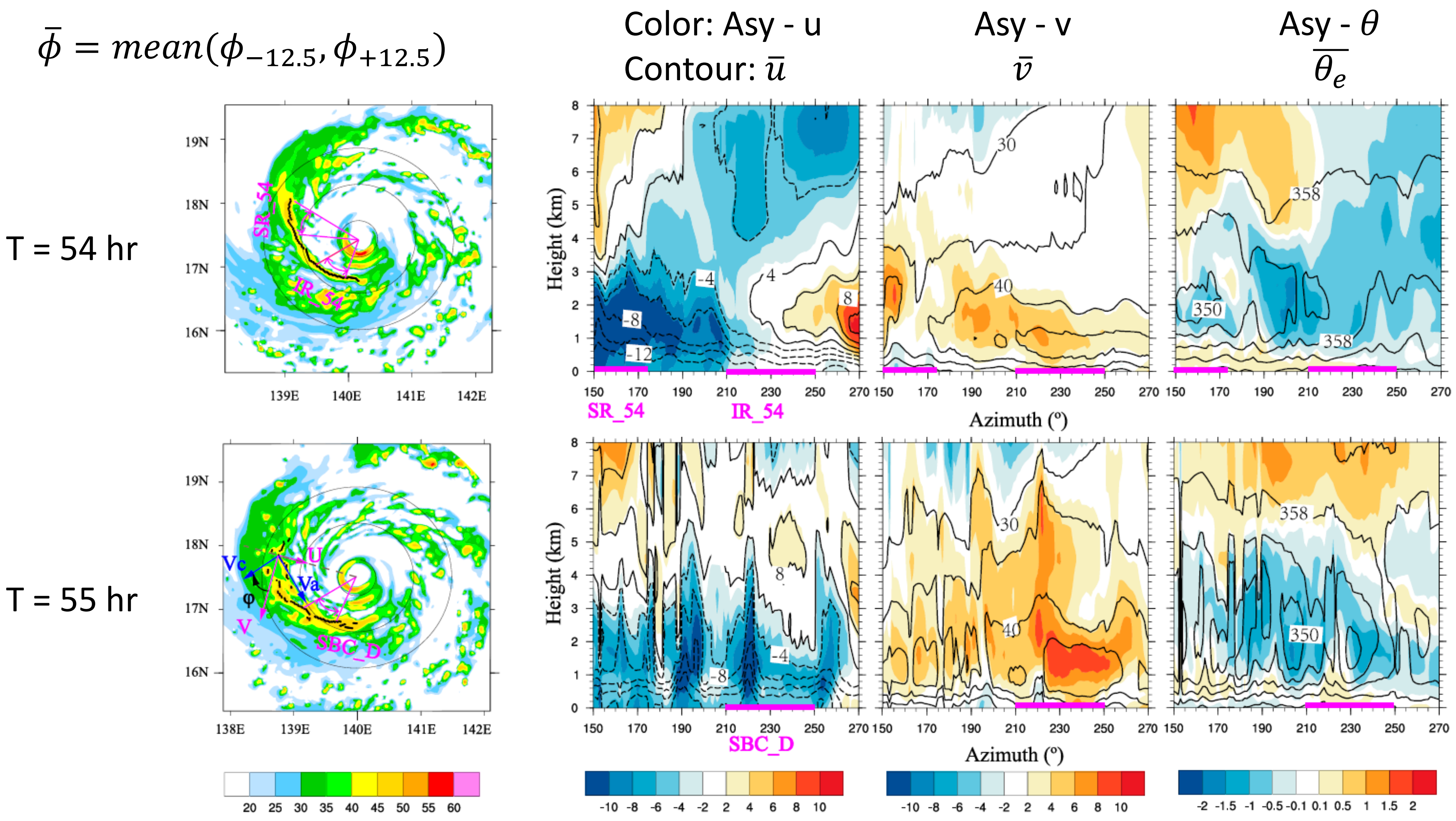

Cold pool formation in the downwind propagation

Average between z = 1 – 3 km
Color: 5x hourly-change θ_e
Circles: 30, 90, 150 km

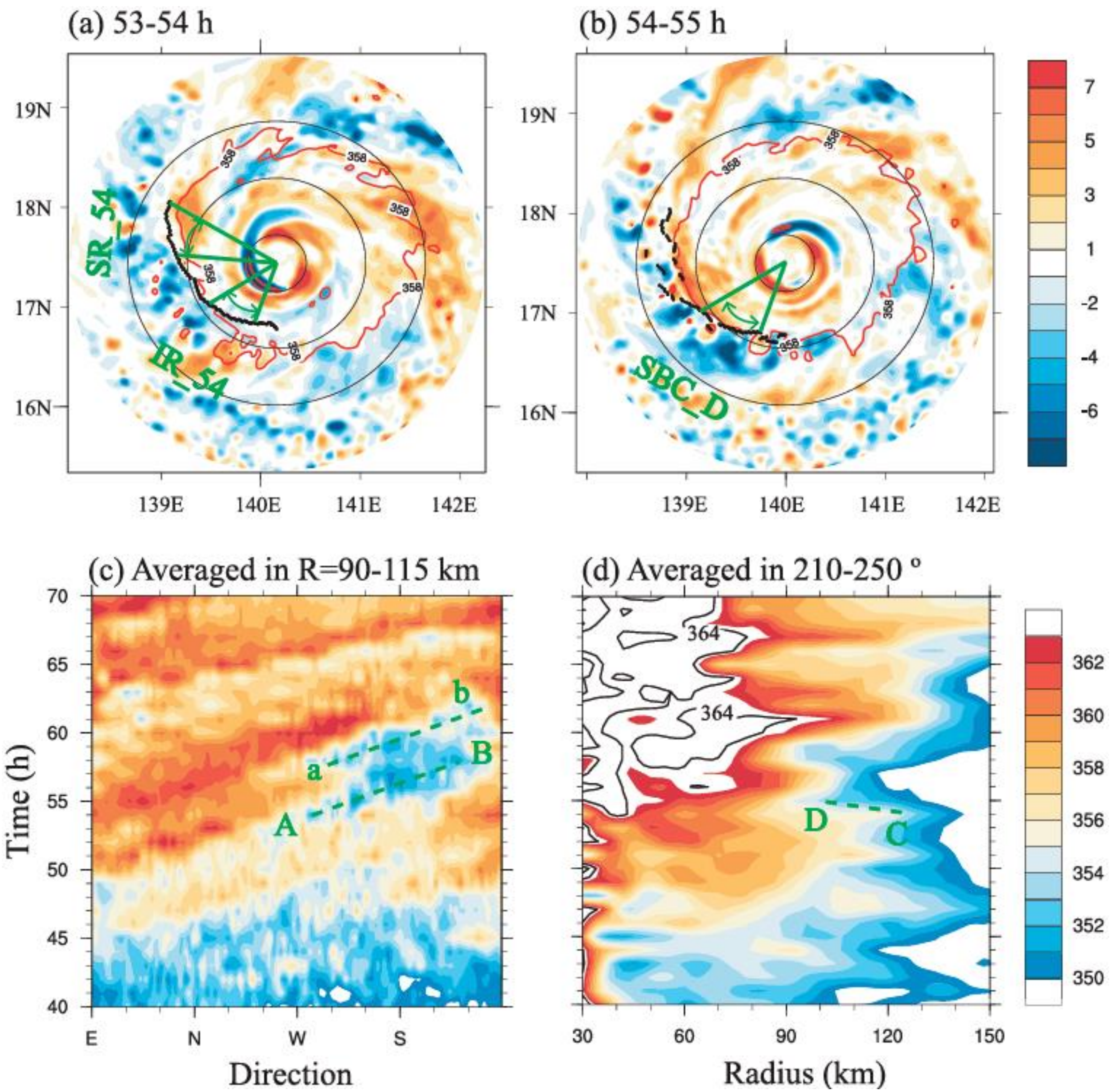

Average between r = 90 – 115 km
(along rainband)
Color: θ_e

Average between
θ = 210 – 250°
(cross rainband)
Color: θ_e

Cold pool formation in the downwind propagation

Average between θ = 210 – 250^o (cross rainband)

Color: Asy - θ_e

Contour: u

Contour: RH

Vector: u, w

T = 54 hr

T = 55 hr

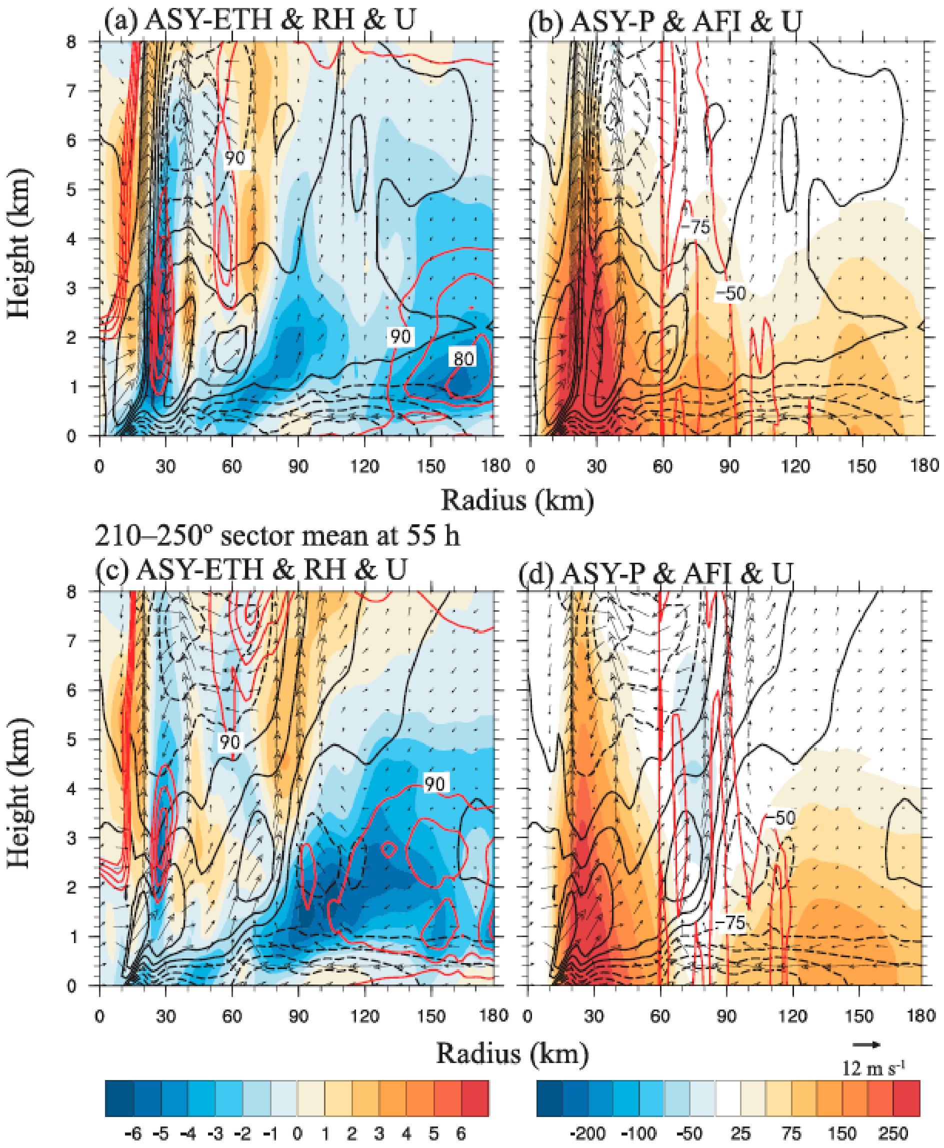

Color: Asy - PGF

Contour: u

Contour: inward PGF

Vector: u, w

Cold pool dynamics in convection enhancement

Line-averaged
Color: θ difference
Contour: w
Vector: cross-band, vertical wind

$\Delta\theta = \theta_{min} - \theta_0$
θ_0: θ before cold pool reached (average within 25-km radial distance in the outward side of rainband)

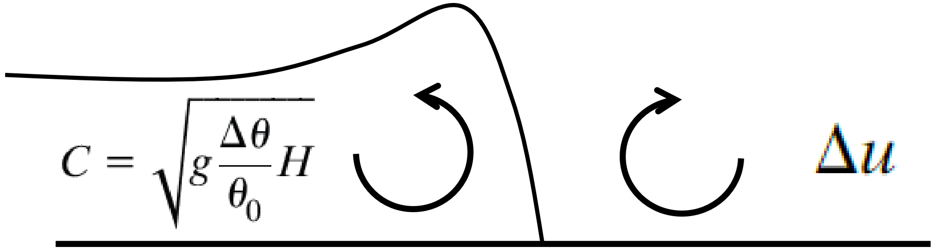

Cross-band wind

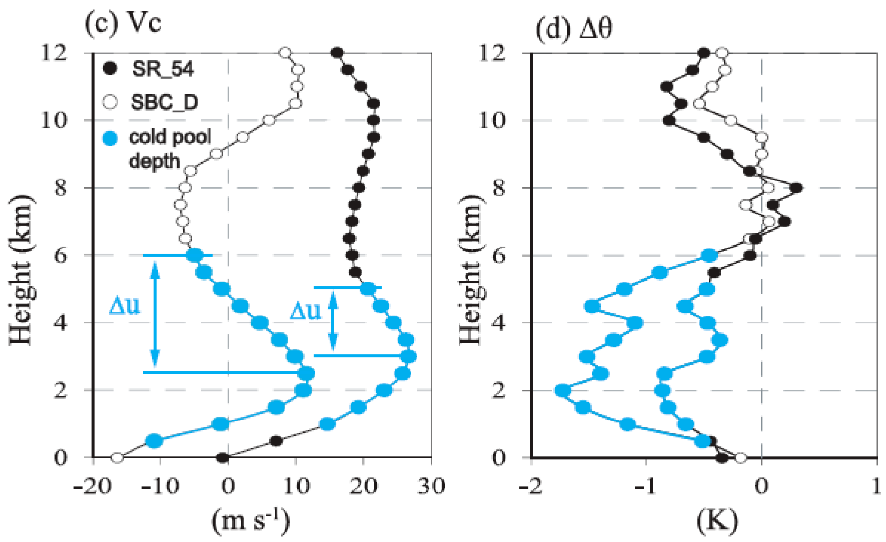

θ difference

	SR_54	SBC_D
θ difference (K)	-1.7 K	-0.9
H (km)	4.0	5.5
C (m/s)	10.8	17.4
Δu (m/s)	-5.5	-16.5
RKW	$C > \Delta u$	$C = \Delta u$

Cold pool formation in the downwind propagation

Cold pool radial speed:

$$V_{cp} = k\sqrt{\frac{gH(\rho_c - \rho_e)}{\rho_e}} + bV_c$$

ρ_c: cold pool density
ρ_e: environmental density
k: 0.9
b: 0.6

	SR_54	SBC_D
H (km)	4.0	5.5
ρ_c (kg/m³)	1.132	1.128
ρ_e(kg/m³)	1.129	1.123
V_c (m/s)	2.88	-13.26
mean V_{cp} (m/s)	-5.19	

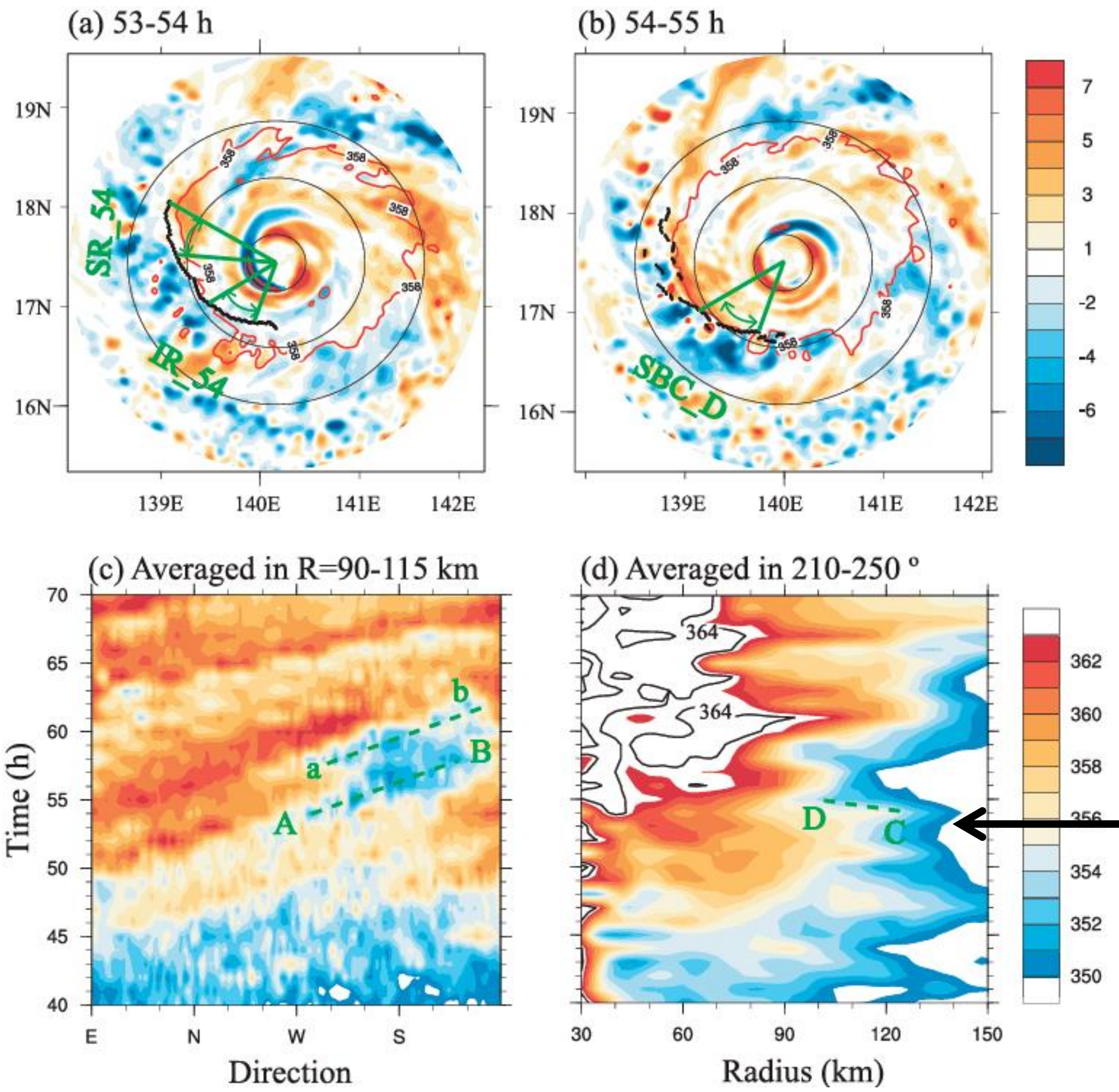

Low-θ_e inward propagation: 7.2 m/s

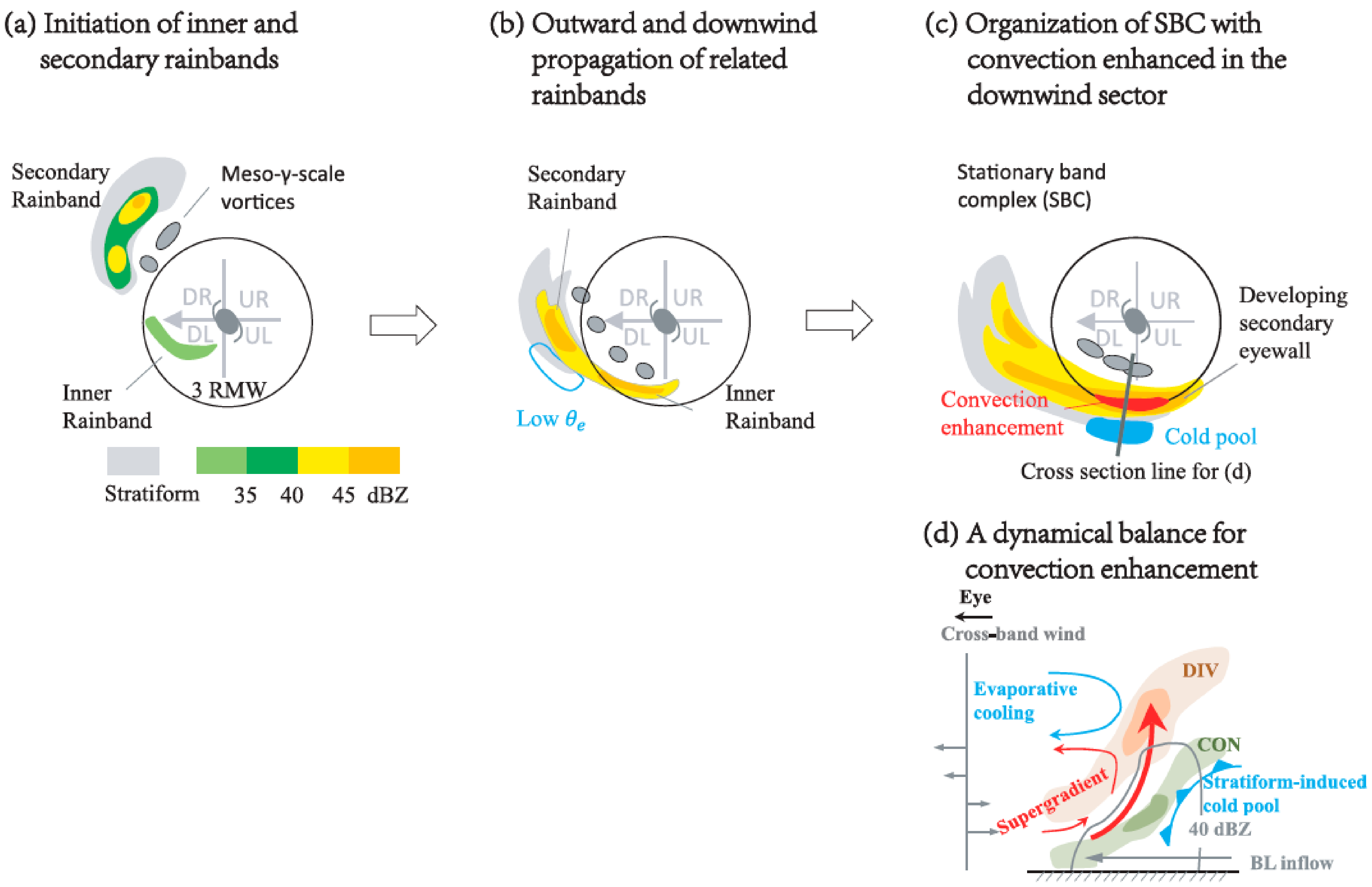

(a) Initiation of inner and secondary rainbands
Secondary Rainband
Meso-γ-scale vortices
DR
UR
DL
UL
Inner Rainband
3 RMW
Stratiform
35
40
45
dBZ
(b) Outward and downwind propagation of related rainbands
Secondary Rainband
DR
UR
DL
UL
Low θe
Inner Rainband
(c) Organization of SBC with convection enhanced in the downwind sector
Stationary band complex (SBC)
DR
UR
DL
UL
Developing secondary eyewall
Convection enhancement
Cold pool
Cross section line for (d)
(d) A dynamical balance for convection enhancement
Eye
Cross-band wind
DIV
Evaporative cooling
CON
Stratiform-induced cold pool
Supergradient
40 dBZ
BL inflow